Nonlinear Dynamics and Neuroscience

Izvestiya Vysshikh Uchebnykh Zavedeniy. Applied Nonlinear Dynamics. 2024;32(5)

Article DOI: 10.18500/0869-6632-003111

Searching the structure of couplings in a chaotic maps ensemble by means of neural networks

A. V. Shabunin

Saratov State University, Russia
E-mail: ✉shabuninav@info.sgu.ru

Received 15.01.2024, accepted 3.03.2024, available online 20.06.2024, published 30.09.2024

Abstract. The *purpose* of this work is development and research of an algorithm for determining the structure of couplings of an ensemble of chaotic self-oscillating systems. *The method* is based on the determination of causality by Granger and the use of direct propagation artificial neural networks trained with regularization. *Results.* We have considered a method for recognition structure of couplings of a network of chaotic maps based on the Granger causality principle and artificial neural networks approach. The algorithm demonstrates its efficiency on the example of small ensembles of maps with diffusion couplings. In addition to determining the network topology, it can be used to estimate the magnitue of the couplings. Accuracy of the method essencially depends on the observed oscillatory regime. It effectively works only in the case of homogeneous space-time chaos. *Discussion.* Although the method has shown its effectiveness for simple mathematical models, its applicability for real systems depends on a number of factors, such as sensitivity to noise, to possible distortion of the waveforms, the presence of crosstalks and external noise etc. These questions require additional research.

Keywords: dynamical chaos, artificial neural networks, ensembles of maps, couplings structure identification.

For citation: Shabunin AV. Searching the structure of couplings in a chaotic maps ensemble by means of neural networks. Izvestiya VUZ. Applied Nonlinear Dynamics. 2024;32(5):636–653. DOI: 10.18500/0869-6632-003111

Introduction

One of the tasks of mathematical modeling is the identification of dynamic systems (DS), i.e. the reconstruction of equations describing the dynamics of a system based on the signals it generates [1–6]. The possibility of its solution is based on Takens' theorem [7]. If the DS is a network of interacting subsystems, the signals from which are available for observation, then the identification task will also include determining the structure of network connections. A number of methods are used to solve it, one of which is based on determining the *Granger causality*

(GC) [8,9]. The GC method allows to identify the influence of one system (**A**ctive) on another (**R**ecepient) by constructing a time forecast of the behavior of the latter with taking into account the dynamics of A and without it. Obviously, taking into account A should either improve the forecast of R, that is, reduce the prediction errors, if A affects R, or leave the forecast accuracy unchanged otherwise. Thus, to determine the GC, two predictor filters are constructed:

$$\begin{aligned} \mathbf{R}(n+1) &= f\left(\mathbf{R}(n), \mathbf{A}(n)\right) \\ \mathbf{R}(n+1) &= g\left(\mathbf{R}(n)\right). \end{aligned} \tag{1}$$

By introducing the average root-mean-square error $\varepsilon = \sqrt{\overline{|\mathbf{R}(n+1)-\mathbf{R}(n)|^2}}$ as a measure of prediction quality, we can determine the degree of influence of A on R as $PI = \left(\varepsilon_g^2 - \varepsilon_f^2\right)/\varepsilon_g^2$ [10].

The GS method and its modifications are used to determine the dependencies between living and nonliving nature systems [11–17]. Its reliability and application features were tested on many models of nonlinear dynamics [18–20]. Despite the apparent simplicity of the algorithm, its practical applicability depends on a number of factors: the noise level of the observed signals, their sparseness in time, the delay between the generated and observed signals, the presence of "hidden" sources that simultaneously affect both analyzed subsystems, etc. Such factors as the dimension of the analyzed system, the complexity of its topology, as well as the choice of prediction algorithm, can play a significant role.

An artificial neural network (ANN) can be used as a tool for determining the structure of couplings of an ensemble of chaotic generators. [21,22]. The ability of a neural network to work as a filter-predictor of chaotic dynamics is well known [23–25]. Accordingly, ANNs can be used as functions f and g in equations (1), thereby implementing the algorithm described above.

An interesting idea was proposed in [26]: taking advantage of the fact that the ANN itself has a network structure, force it to adjust its own structure of synaptic connections to the structure of the ensemble couplings during training, thereby identifying the latter. This task can be considered as a structural optimization problem. In the initial state, an untrained ANN is fully connected. Such architecture may be redundant for successfully predicting the dynamics of the analyzed system.

Is it possible to force a neural network to "remove" unnecessary connections during training? A similar method is known and has long been used for other purposes — preventing overtraining of the network. It is based on the introduction of a "complexity penalty" that ensures maximum simplification of the network structure with an acceptable level of its efficiency. This method is called *training with regularization* [21]. The regularization method was first proposed by A. N. Tikhonov [27] and has been widely used in optimization problems.

When using structural optimization that occurs during the training of the ANN to predict the chaotic dynamics of the ensemble, the intensity of the synaptic coefficients takes the minimum necessary values, sufficient for a successful prediction. These values, properly normalized, can be used to assess the presence of couplings between the elements of the ensemble and their intensity. This method is an alternative to using the standard criterion in the form of a PI factor.

In this paper, we propose an algorithm for estimating the structure of connections of an ensemble of chaotic mappings based on the [26] method. The algorithm is tested on several simple examples — chains of identical one-dimensional mappings with unidirectional and mutual diffusion connections, for which its performance is demonstrated. The paper also determines the sensitivity of the method to the choice of the regularization parameter and studies the possibility of using it to estimate the magnitude of connections.

1. The ensembles under study

Let a self-oscillating system be defined by a discrete-time map $x(n+1) = f(x(n))$, where x is a real dynamic variable describing the state of the system at time n; f is a function defining its change at one step of discrete time. Let us consider an ensemble of N identical interacting systems:

$$x_i(n+1) = f(x_i) + \sum_{j=1}^{N} C_{ij} \left(f(x_j) - f(x_i) \right), \; i = 1, ..., N. \tag{2}$$

Here the subscript is the number (identifier) of the ensemble element, and the matrix $\hat{C}$ specifies the topology and intensities of the couplings between the maps. The term in brackets is a discrete analogue of the operator ∇. Therefore, this type of couplings is called *the diffusion coupling* ([28, 29]). To simplify the problem, we will assume that the strengths of all couplings are the same. In this case, the matrix $\hat{C}$ takes the form $\gamma\hat{L}$, where γ is the common coupling coefficient for all elements, and the *adjacency matrix* $\hat{L}$ specifies their structure: the element L_{ij} takes the value 1 if node j affects node i, and the value 0 if there is no such effect.

It is convenient to rewrite the system of equations (2) in matrix-vector form. To do this, we define a column vector $\mathbf{x} = [x_1, x_2, \ldots, x_N]^T$, where the superscript T denotes transposition. Then we obtain the equation

$$\mathbf{x}(n+1) = \hat{M}\mathbf{f}\left(\mathbf{x}(n)\right), \tag{3}$$

where $N \times N$ matrix $\hat{M}$ is the general matrix of ensemble couplings. It takes into account mutual influences of oscillators on each other and self-interactions: diagonal elements $M_{ii} = 1 - q\gamma$, where $q \in [0, N-1]$ is the number of other nodes acting on the i-th, and off-diagonal $M_{ij} = \gamma L_{ij}$. Determining the matrix $\hat{M}$ based on observations of the ensemble dynamics is the task of this study.

Let us choose as an element of the ensemble (2) the logistic map defined by the equation

$$x(n+1) = \alpha x(n)\left(1 - x(n)\right), \tag{4}$$

where $\alpha \in [0:4[$ is a parameter. The (4) map is one of the basic models of nonlinear dynamics, whose behavior is well known. Depending on α, it can exhibit various regular and chaotic regimes: a fixed point (periodic oscillations) with a period of one, oscillations with a period of 2^k ($k = 1, 2, 3, ...$), weak (coherent) chaos in the form of multi-band chaotic attractors, and developed incoherent chaos. The last regime ($\alpha = 3.95$) is chosen by us as the initial one.

When combining (4) maps into an ensemble, the oscillation regime, in addition to α, is also determined by the parameter γ and the matrix $\hat{L}$. Accordingly, under certain couplings it can change from chaotic to regular. Such cases will be excluded from consideration.

2. Using ANN to Estimate the Ensemble Link Matrix

Determining the structure of ensemble couplings is closely related to the problem of system identification, which is solved using multilayer direct propagation neural networks trained with a teacher [21]. The simplest version of such a network is a two-layer network with a nonlinear and monotone activation function of the first layer and a linear output layer (Fig. 1), the equation of which has the form

$$\mathbf{Y}_1 = \boldsymbol{\varphi}\left(\hat{W}\mathbf{X} + \mathbf{b}_1\right), \quad y = \hat{U}\mathbf{Y}_1 + b_2. \tag{5}$$

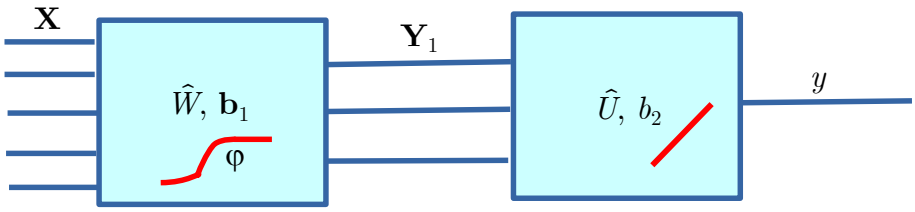

Fig 1. The scheme of a two-layer neural network

Here y is a scalar signal at the network output, $\mathbf{X} = [X_1, X_2, ..., X_N]^T$ is an N-dimensional vector of the input signal, $\mathbf{Y}_1 = [Y_1, Y_2, ..., Y_M]^T$ is an M-dimensional vector of the first layer output signal, $\hat{W}$ and $\hat{U}$ are $M \times N$ and $1 \times M$ matrices of weight coefficients (*synaptic weights*) of neurons of the first and second layers, respectively, and $M \times 1$ vector $\mathbf{b}_1$ and b_2 are their biases; $\boldsymbol{\varphi}(\mathbf{x}) = [\varphi_1(\mathbf{x}), \varphi_2(\mathbf{x}), \ldots, \varphi_M(\mathbf{x})]^T$ — vector sigmoid activation function of the first layer in the form of hyperbolic tangent, acting elementwise on each component of its argument according to the rule $\varphi_i(\mathbf{x}) = \tanh(x_i)$. Since the ANN is used as a predictor filter for the system (2), its input dimension (N) should be equal to the dimension of the ensemble. The intermediate dimension (M) can be chosen arbitrarily and is determined by the complexity of the problem and the accuracy of the approximation. In this study, the value $M = 10$ is used.

To identify the system (2, 4), we will use the *supervised learning* method, where the vector $\mathbf{x}(n)$ at the current time is taken as the input signal, and the scalar signal from the i-th node $x_i(n+1)$ is taken as the target value. Thus, the goal of learning is to predict the dynamics of the i-th mapping one step ahead. The essence of learning is to optimize the network parameters that minimize the target function $\boldsymbol{\Phi}\left(\hat{W}, \mathbf{b}_1, \hat{U}, b_2\right)$. As a rule, the mean square of the prediction errors is chosen as the latter $\varepsilon(n) = y(n) - x_i(n+1)$:

$$\boldsymbol{\Phi}_{\text{err}} = \frac{1}{K}\sum_{n=1}^{K}\varepsilon^2(n), \tag{6}$$

where $K \gg 1$ is the number of training vectors, i.e. the duration of observation of the ensemble dynamics.

If the learning is successful, i.e. $\boldsymbol{\Phi}_{\text{err}} \simeq 0$, the neural network correctly predicts the dynamics of the corresponding (i-th) map of the ensemble based on the previous data obtained from all maps. Does this mean that the structure of connections within neural layers follows the structure of couplings between oscillators in the ensemble? As will be shown below, no such correspondence is observed.

The reason is that the target function (6) used during training only estimates the accuracy of the system approximation (2, 4), but is in no way related to the structure of the neural network itself. In order for the ANN to adapt to the ensemble structure during training, in addition to the existing training aim — reducing prediction errors — it is necessary to also require a simultaneous simplification of the structure of the neural network itself, that is, removing from it ("zeroing") synaptic coefficients that are unnecessary for successful approximation. To solve this problem, following the recommendations of [26], we add to the target function (6) a "complexity penalty", which is the sum of the squares of the synaptic coefficients of the entire network:

$$\boldsymbol{\Phi}_{\text{cp}} = \sum_{k=1}^{2}\sum_{ij} W_{ij,k}^2, \tag{7}$$

where k is the layer number, i, j are the row and column numbers of the corresponding matrices. The new objective function will be a weighted sum (6) and (7):

$$\mathbf{\Phi} = \mathbf{\Phi}_{\text{er}} + r\mathbf{\Phi}_{\text{cp}}, \tag{8}$$

where the weighting coefficient $r \geqslant 0$ is called the *regularization coefficient* (RC). RC defines the relationship between the two learning goals: the ability to predict the ensemble dynamics and the reduction of the required synaptic coefficients of the ANN.

Thus, the method for diagnosing the structure of couplings of an ensemble of maps is as follows:

1. An ANN is created, the structure of which is shown in Fig. 1, with an input dimension equal to the number of ensemble elements N, and the number of neurons in the hidden layer $M = 10$.
2. The network coefficients are initialized with random values uniformly selected from the interval $[-1, 1]$.
3. To train the ANN, a training set of $K = 5000$ vectors $\left\{\mathbf{X}^{(n)}\right\}_{n=0}^{K-1}$ is formed, each of which represents a map of the entire ensemble at the n-th moment in time: $\mathbf{X}^{(n)} = \mathbf{x}(n)$.
4. A set of target values $\left\{y_i^{(n)}\right\}_{n=0}^{K-1}$ is formed, i.e. $y_i^{(n)} = x_i(n+1)$.
5. The network is trained with regularization based on the target function (8). Training can be performed using the backpropagation method using gradient methods. In this work, the quasi-Newton algorithm, which is a second-order method, was used for faster convergence. The following values of the algorithm's operating parameters were chosen: the minimum value of the target function $\mathbf{\Phi}_{\min} = 10^{-6}$; the minimum value of the objective function gradient modulus $|\nabla\mathbf{\Phi}|_{\min} = 10^{-6}$; the maximum number of training epochs was 3000.
6. To identify couplings, the matrix of synaptic coefficients of the first layer $\hat{W}$ is used, the columns of which correspond to the numbers of network inputs (i.e., the numbers of ensemble oscillators). To quantitatively determine the degree of influence of the j-th oscillator on the prediction of the dynamics of the i-th, the root-mean-square value of the coefficients of the j-th column is calculated

$$w_{ij} = \frac{1}{M}\sqrt{\sum_{k=1}^{M} W_{kj}^2},$$

which is then normalized to the sum of such values for all columns:

$$S_{ij} = \frac{w_{ij}}{\sum_{l=1}^{N} w_{il}}. \tag{9}$$

The obtained values S_{ij} will be called *influence coefficients* of the j-th node on the i-th, and the matrix $\hat{S}$ composed of them will be called the *influence matrix*. The latter will be used to identify the structure of the ensemble's couplings.

3. Definition of the structure of couplings of the ensemble of logistic maps

Using the algorithm described in the previous section, we will estimate the structure of couplings in the ensemble (4), gradually complicating the task.

3.1. Two maps with unidirectional coupling. Let us first consider the simplest case — two maps with a unidirectional coupling

$$x_1(n+1) = f\left(x_1(n)\right)$$
$$x_2(n+1) = f\left(x_2(n)\right) + \gamma\left(f\left(x_1(n)\right) - f\left(x_2(n)\right)\right). \tag{10}$$

The coupling matrix for (10) is

$$\hat{M} = \begin{bmatrix} 1 & 0 \\ \gamma & 1-\gamma \end{bmatrix}. \tag{11}$$

At the selected parameter $\alpha = 3.95$ the ensemble demonstrates the regime of developed chaos in the entire considered interval $0 \leqslant \gamma \leqslant 0.5$. This is confirmed by the values of the Lyapunov exponents (Fig. 2, *a*). At the same time, in the region $0 \leqslant \gamma < 0.33$ (marked in light gray) the hyperchaos regime is observed, and at $\gamma > 0.436$ — the regime of complete chaotic synchronization (marked in gray).

We choose the value $\gamma = 0.12$, corresponding to the asynchronous chaotic regime, the phase portrait of which is shown in Fig. 2, *b*, and train the ANN to predict the dynamics of the first oscillator. First, we train without regularization, that is, at $r = 0$. The network is trained successfully, as evidenced by the smallness of the mean square error $\Phi_{\text{err}} < 10^{-6}$. The values of the synaptic coefficients of the first and second layers of the ANN obtained as a result of training are displayed in Table 1a.

To analyze connectivity, we will use the matrix of coefficients of the first layer, that is, the vectors $\mathbf{W}_1$ and $\mathbf{W}_2$. It is clear from Table 1a that they do not correspond to the matrix of connections (11), since the values of the coefficients of the second column ($\mathbf{W}_2$), determining the influence of the second network input on the output signal, are by no means small, but are comparable in magnitude with the coefficients of the first column ($\mathbf{W}_1$): the mean square values of the coefficients for both inputs are 3.12 and 2.36, respectively. Similar results are obtained when training the ANN to predict the dynamics of the second mapping (Table 1b). In this case, the mean square values of the coefficients for both inputs are almost equal: 2.68 and 2.62. Thus,

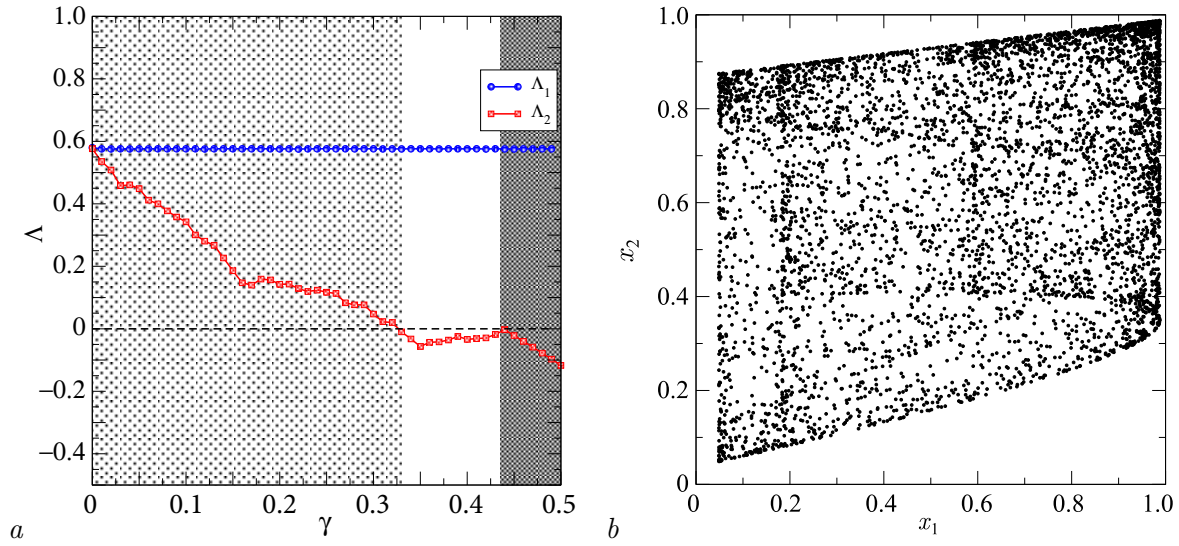

Fig 2. System dynamics (10) at $\alpha = 3.95$: *a* — plots of Lyapunov exponents in dependence of γ; *b* — phase portrait at $\gamma = 0.12$ (color online)

Table 1. Matrices of synaptic coefficients of the first ($\mathbf{W}_1$, $\mathbf{W}_2$) and second ($\mathbf{U}_1^{(T)}$) ANN layers trained to predict the dynamics of the first (a) and the second maps (b); the regularization parameter $r = 0$

	$\mathbf{W}_1$	$\mathbf{W}_2$	$\mathbf{U}_1^{(T)}$		$\mathbf{W}_1$	$\mathbf{W}_2$	$\mathbf{U}_1^{(T)}$
	−2.0798	0.0027	2.1324		0.1227	−2.1740	1.6062
	2.4799	−3.4474	0.2769		2.3330	1.0260	−0.2417
	−0.8994	4.3298	−0.2313		−3.3696	−1.4181	−0.0895
	2.6254	0.0041	0.9538		−0.6316	4.2700	−2.6671
a	−3.8335	−1.8255	−0.0099	b	0.1671	−2.4699	−1.1406
	−4.4584	0.0720	−1.2758		−2.8242	−3.2945	−0.5918
	−4.2626	−1.1638	−0.1892		−3.025	−2.0144	−0.7058
	−2.8823	−3.3587	−0.0315		4.197	1.4731	−0.0585
	3.5911	−2.4527	0.0782		3.9470	1.9978	0.1933
	2.3295	−1.7919	−2.4551		2.0082	3.9453	0.4832

in the absence of regularization, we do not see a significant difference between the values of the coefficients $\mathbf{W}_1$ and $\mathbf{W}_2$. This means that the ANN does not adjust its own connection structure to the ensemble structure and cannot be used to estimate the latter.

Let us now consider training an ANN with regularization. We choose a sufficiently small value of the regularization coefficient, $r = 10^{-4}$, and train the network again. The new values of the synaptic coefficients of the trained ANN for the first and second maps are presented in tables 2a and 2b, respectively. Let us consider table 2a. Here the coefficients of the first and second columns differ by two orders of magnitude: for the first layer, the mean square of the coefficients is 0.99, and for the second, only 0.009. Based on the values of the coefficients $\mathbf{W}_2$,

Table 2. Matrices of synaptic coefficients of the first ($\mathbf{W}_1$, $\mathbf{W}_2$) and second ($\mathbf{U}_1^{(T)}$) ANN layers trained to predict the dynamics of the first (a) and the second map (b); the regularization parameter $r = 0.0001$

	$\mathbf{W}_1$	$\mathbf{W}_2$	$\mathbf{U}_1^{(T)}$		$\mathbf{W}_1$	$\mathbf{W}_2$	$\mathbf{U}_1^{(T)}$
	0.0285	−0.0023	−0.3762		0.2392	0.0040	−0.5196
	0.0298	0.0097	−0.1169		−0.2426	0.0160	0.5004
	2.1769	−0.0007	−1.8684		0.2493	−0.0322	−0.6014
	0.0065	−0.0068	−0.3424		0.0018	−2.0389	1.7979
a	−0.0279	0.0041	0.2610	b	0.0029	−2.1686	−1.4956
	−2.2665	−0.0008	−1.6906		−0.2423	0.0182	0.5939
	−0.0241	−0.0096	0.3830		−0.2463	0.0208	0.4664
	−0.0218	0.0190	0.3879		1.3376	0.0094	0.8936
	−0.0323	−0.0087	0.4603		0.2419	−0.0103	−0.4914
	0.0299	0.0099	−0.4659		0.2449	−0.0157	−0.4937

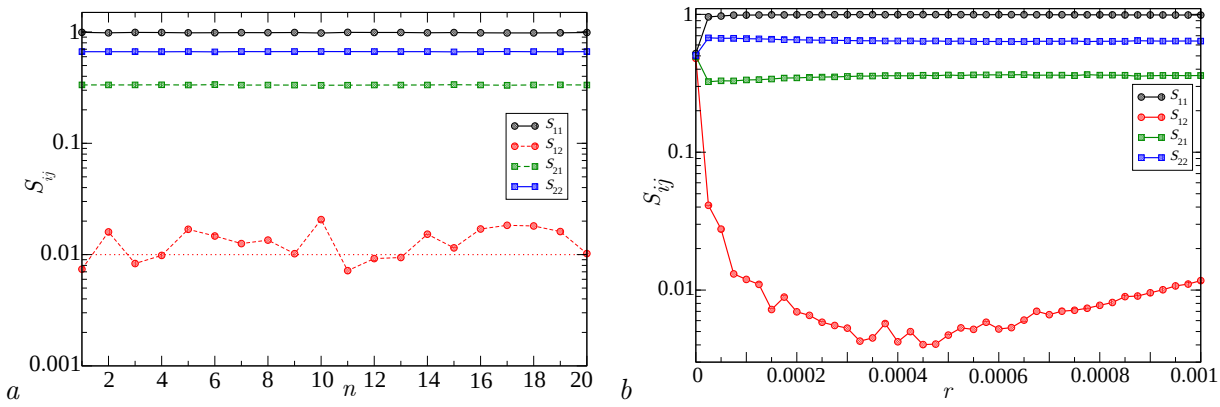

Fig 3. The dependence of the influence coefficients S_{ij} on the number of the training attempt n (a) and on the regularization parameter (b) (color online)

we can conclude that the influence of the second map on the dynamics of the first is either very small or absent altogether. When training an ANN to predict the dynamics of the second map, the difference in the values of the coefficients $\mathbf{W}_1$ and $\mathbf{W}_2$, as can be seen from Table 2b, is not so significant. The obtained results are also reproduced during repeated training, as evidenced by the series of coefficients S_{ij} presented in Fig. 3, *a*, obtained from twenty separate trainings. During each test, the neural network was reinitialized, after which it was retrained on the same training set. From the graphs it is clear that (a) the results are repeated with an accuracy of about one percent; (b) the influence of the second oscillator on the dynamics of the first (S_{12}) in all cases remains around one percent, while the influence of the first on the second (S_{21}) is around 34%.

Let us estimate the influence of the regularization coefficient on the values of S_{ij}. To do this, we will train the ANN for different values of r and plot the graphs of the dependencies $S_{ij}(r)$. The calculation results are shown in Fig. 3, *b* in a logarithmic scale along the ordinate axis. It is more convenient to analyze them using the example of S_{12}, since the exact value for it is zero. From the calculations performed, it follows that for $r \in [0.0001, 0.001]$ the value of the coefficient S_{12} does not exceed one percent. The dependence $S_{12}(r)$ reaches a minimum at $r \simeq 0.00045$, amounting here to about 0.5 percent. The values of the remaining influence coefficients at $r > 0.000025$ remain almost unchanged and in the considered range take the values $S_{11} \simeq 1$, $S_{22} \simeq 0.64$, $S_{21} \simeq 0.36$. Based on the analysis, we can conclude that any values of the KR in the range from 0.0001 to 0.001 are acceptable for calculating the influence coefficients. For further calculations, we will use $r = 0.0003$.

Thus, the procedure of training the ANN with regularization allows us to obtain the matrix of influence coefficients presented in table 3, which qualitatively corresponds to the matrix of ensemble connections (11). As for the quantitative correspondence, it will be discussed further.

Table 3. The matrix $\hat{S}$ for system (10), obtained from the results of training the ANN with the regularization parameter $r = 0.0003$

0.996	0.004
0.36	0.64

4. Comparison of the PCA Array with the Mean Field Model

4.1. An ensemble of six maps. Let us now consider a system similar in structure, but of greater dimension — an ensemble of six unidirectionally coupled maps:

$$\begin{aligned} x_1(n+1) &= f\left(x_1(n)\right), \\ x_i(n+1) &= f\left(x_i(n)\right) + \gamma\left(f\left(x_{i-1}(n)\right) - f\left(x_i(n)\right)\right), \\ i &= 2 \ldots 6 \end{aligned} \tag{12}$$

with a matrix of couplings

$$\hat{M} = \begin{bmatrix} 1 & 0 & \ldots & 0 \\ \gamma & 1-\gamma & \ldots & 0 \\ & \ldots & & \\ 0 & 0 & \gamma & 1-\gamma \end{bmatrix}. \tag{13}$$

The dynamics of this ensemble is similar to the dynamics of the two maps. With the chosen α, it exhibits a regime of developed temporal chaos, which becomes synchronous with $\gamma \geqslant 0.436$. This is confirmed by the graphs of the Lyapunov characteristic exponents shown in Fig. 4.

From their comparison with the graphs in Fig. 2, *a*, the similarity in the behavior of both systems is clearly visible.

Let us choose the same value of the coupling parameter $\gamma = 0.12$ as for the system (10) and train the ANN at $r = 0.0003$. The influence coefficients S_{ij} obtained as a result of training are given in the table 4 and are presented as a map in Fig. 5, *a*. As can be seen from the figure, the structure of the matrix $\hat{S}$ for the ensemble (12), as well as for the simpler system (10), qualitatively corresponds to the matrix $\hat{M}$. Thus, the white cells on the map 5, *a* correspond to zero, the black ones to one, and the gray ones to the remaining coefficients of the matrix

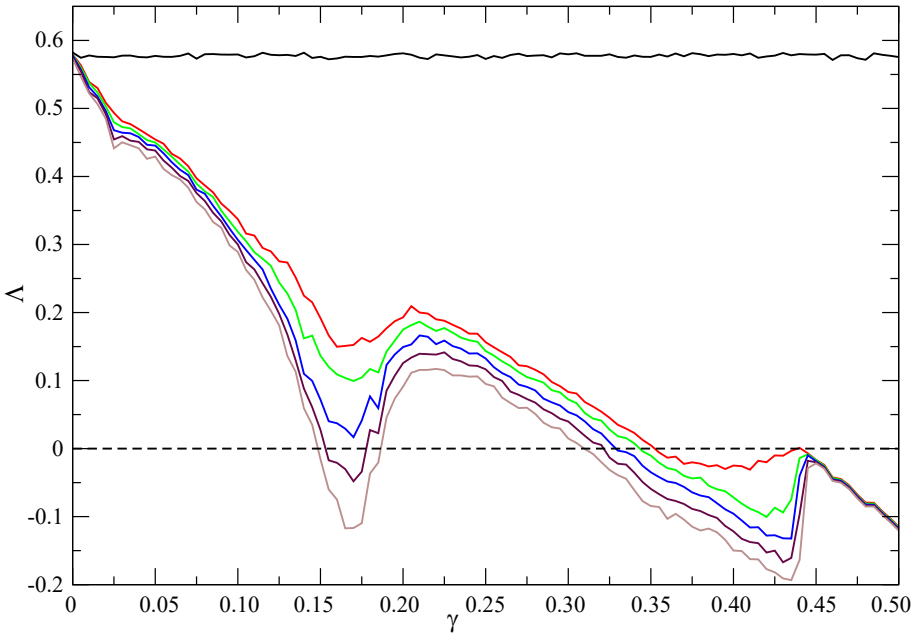

Fig 4. Dependence of Lyapunov exponents on γ for system (12) (color online)

Table 4. Matrix $\hat{S}$ for system (12), obtained from the results of training the ANN with the regularization parameter $r = 0.0003$

0.9617	0.0090	0.0067	0.0073	0.0079	0.0073
0.3256	0.6264	0.0117	0.0102	0.0154	0.0108
0.0055	0.3350	0.6245	0.0097	0.014	0.0113
0.0053	0.0068	0.3426	0.6283	0.0083	0.0087
0.0077	0.0096	0.0081	0.3423	0.6251	0.0071
0.0080	0.0083	0.0124	0.0074	0.3404	0.6235

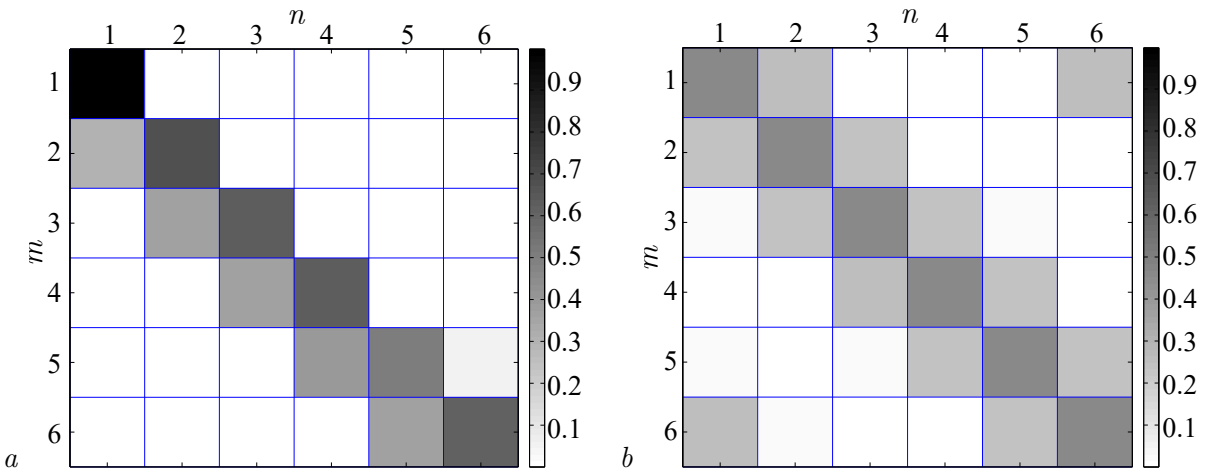

Fig 5. Visual representation of $\hat{S}$ influence matrix as a map for ensemble (12) (a) and ensemble (14) (b)

(13). Thus, increasing the ensemble dimension did not lead to deterioration of the method's performance, which still confidently recognizes the structure of the system's connections.

4.2. Ensemble with symmetrical couplings. Let us now turn to the case where an ensemble element can have several connections. One such system is a ring of six oscillators with symmetric couplings:

$$x_i(n+1) = f\left(x_i(n)\right) + \gamma\left(f\left(x_{i-1}(n)\right) + f\left(x_{i+1}(n)\right) - 2f\left(x_i(n)\right)\right) \tag{14}$$

$$i = 1 \ldots 6.$$

The matrix of the cyclic couplings is

$$\hat{M} = \begin{bmatrix} 1-2\gamma & \gamma & \ldots & \gamma \\ \gamma & 1-2\gamma & \ldots & 0 \\ & \ldots & & \\ \gamma & 0 & \gamma & 1-2\gamma \end{bmatrix}. \tag{15}$$

The system (14) demonstrates a much greater diversity of modes than ensembles with unidirectional connections. In particular, for the chosen α, both chaotic and regular modes can be observed here, depending on the intensity of the couplings. This is confirmed by the graphs of the two highest Lyapunov exponents (Fig. 6), which were calculated for $\alpha = 3.95$. The previously chosen value $\gamma = 0.12$ here also corresponds to the mode of chaotic oscillations, so it can be used in the analysis of connectivity. For small γ, the ensemble (14) demonstrates multistability, so when

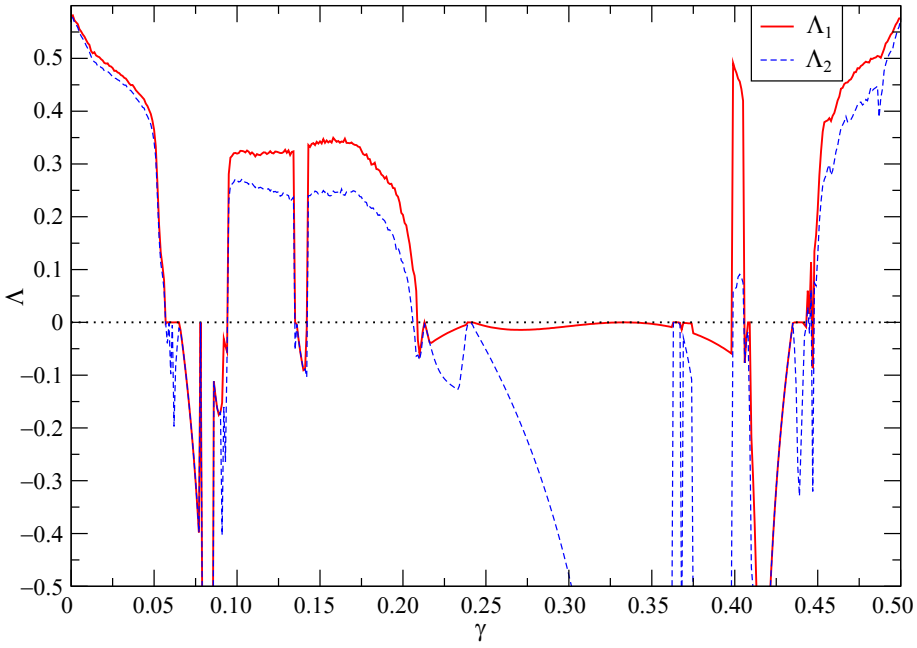

Fig 6. The dependence of the two largest Lyapunov exponents from γ in system (14) (color online)

conducting studies, in addition to the parameters, it is necessary to control the initial conditions. The latter were chosen in a small neighborhood of the symmetric subspace: $\mathbf{x}_0 = 0.1 + 0.001\boldsymbol{\xi}$, where $\boldsymbol{\xi}$ is a random vector of unit length.

Let us calculate the influence coefficients using the same method as before. As a result, we obtained the coefficients S_{ij}, which are displayed in the table 5, and are also presented in Fig. 5, *b* as a map. From the comparison of the obtained matrix $\hat{S}$ with the matrix of connections $\hat{M}$ (15), their qualitative correspondence is clearly visible.

Thus, ANNs trained to predict the dynamics of an ensemble of chaotic maps adjust, under regularization, the values of synaptic coefficients to the structure of the ensemble's connections, thereby allowing the latter to be determined. The method works for small ensembles with both unidirectional and mutual couplings.

Table 5. Matrix $\hat{S}$ for system (14), obtained from the ANN training with the regularization parameter $r = 0.0003$

0.4628	0.2506	0.0123	0.0085	0.0150	0.2509
0.2488	0.4654	0.2494	0.0118	0.0093	0.0152
0.0182	0.2437	0.4644	0.2447	0.0166	0.0124
0.0088	0.0133	0.2509	0.4645	0.2495	0.0130
0.0176	0.0099	0.0165	0.2486	0.4595	0.2480
0.2497	0.0164	0.0090	0.0152	0.2464	0.4633

5. Estimation of the values of the coupling coefficient

The previous sections considered the issue of determining the network topology. Can the proposed method also be used to estimate the magnitude of the coupling coefficient? To answer this question, we will calculate the influence coefficients depending on the coupling parameter γ and analyze the obtained dependencies.

Let us first consider the simplest case — a system of two maps (10) — and calculate the graphs $S_{ij}(\gamma)$ for it. The results of the calculations are presented in Fig. 7, *a*. Let us analyze the obtained dependencies. We see that in the entire interval from $\gamma \simeq 0$, up to the value $\gamma \simeq 0.436$, the values of the coefficients S_{11} and S_{12} are close to the values one and zero, respectively. Thus, in this interval $S_{11} \simeq M_{11}$ and $S_{12} \simeq M_{12}$. At $\gamma \simeq 0.436$, the system (10) transits to the mode of complete synchronization of chaos, simultaneously with which the influence coefficients, as can be seen from the graphs, abruptly change their values up to $S_{11} \simeq S_{12} \simeq 0.5$. Accordingly, upon transition to the zone of chaotic synchronization, which is in Fig. 7, *a* is marked in gray, the algorithm stops working.

Let us now turn to the two remaining coefficients. Since they are related by the relation $S_{21} + S_{22} = 1$, we will limit ourselves to analyzing one of them — S_{21}. It is clearly seen from Fig. 7, *a* that in the region of asynchronous chaos $S_{21}(\gamma)$ is a smooth monotonically increasing coupling function, the shape of which resembles the power dependence $S_{21} \sim A\gamma^p$ for $p < 1$. To test this hypothesis, we will plot $S_{21}(\gamma)$ on a logarithmic scale (Fig. 7, *b*), in which the power functions look like straight lines. Indeed, from the graph's appearance, it can be concluded that in the range $0.01 < \gamma < 0.436$ the dependence $S_{21}(\gamma)$ is close to a power function. The selection of the coefficients A and p, carried out using the least squares method, leads to the relation

$$S_{21} \simeq 0.57\sqrt[4]{\gamma}, \tag{16}$$

This is shown in Fig. 7, *a* and 7, *b* by the dotted line. The presence of an unambiguous relationship between S_{21} and γ seems quite trivial. However, its simple form seems to be an interesting result, the reasons for which are not entirely clear at the moment. Nevertheless, for the system under consideration, the expression (16) allows us to estimate the coupling coefficient based on the values of the synaptic coefficients of the trained neural network.

Let us now consider the case of a higher-dimensional ensemble (13), plotting the same graphs as in the previous case. The calculation results are shown in Fig. 8, *a*, where the graphs

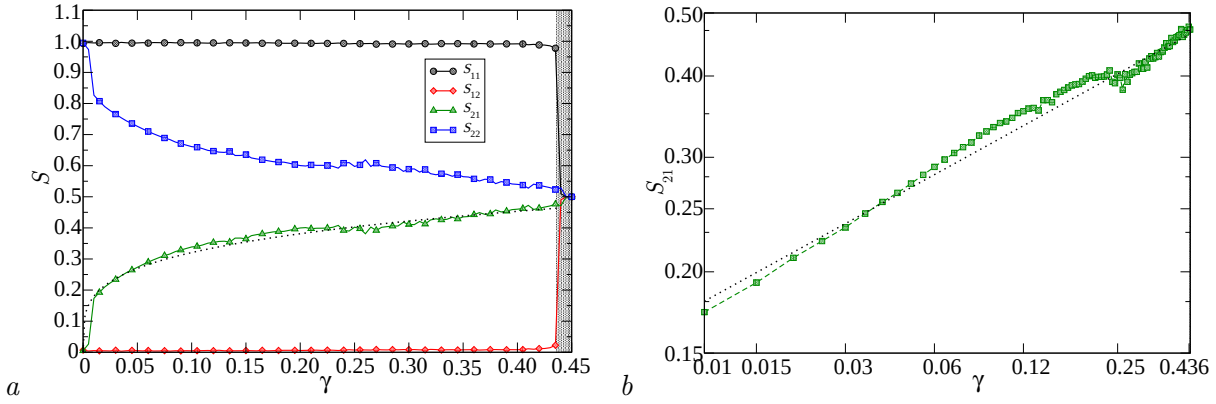

Fig 7. The dependence of the coefficients of influence on γ for the system (10) in linear (*a*) and logarithmic (*b*) scales (color online)

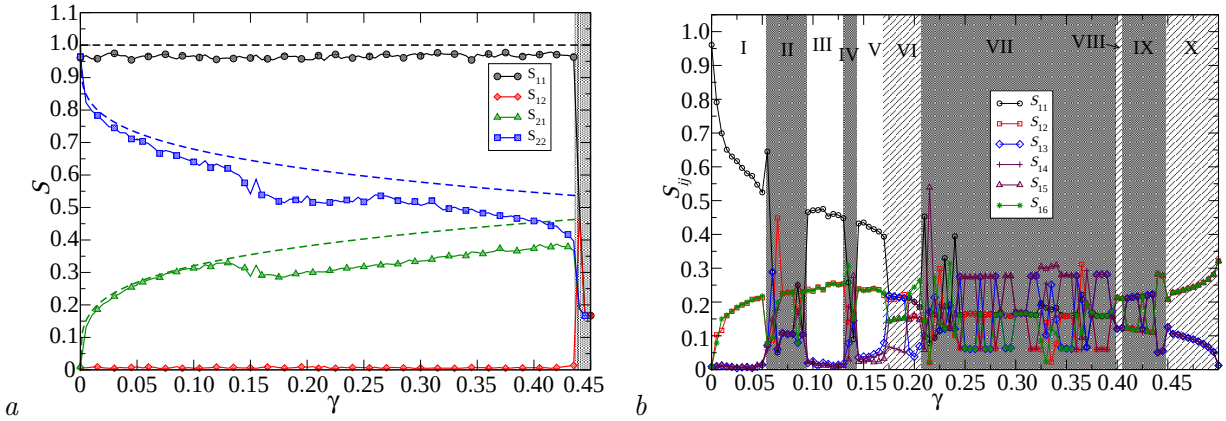

Fig 8. Plots $S_{ij}(\gamma)$ for system (12) (*a*) and system (14) (*b*) (color online)

for a two-dimensional system are shown by dashed lines for comparison. As can be seen from the comparison, there is a significant similarity between the $S_{ij}(\gamma)$ dependencies, along with some minor differences. Thus, for $\gamma \lesssim 0.13$, the $S_{21}(\gamma)$ graph almost coincides with the approximating curve (16) in the range $0.15 \lesssim \gamma < 0.436$ and lags behind it by ~ 0.1. The reason for this difference is not entirely clear. One can only assume that it is related to the change in the structure of the chaotic attractor, which occurs at $\gamma \simeq 0.15$; the latter can be seen from the sharp decrease in the magnitude of the transversal Lyapunov exponents (Fig. 4). If this hypothesis is correct, it means that the accuracy of the estimate of the magnitude of the connections should be related to the degree of chaos in the dynamics of the subsystems and deteriorate in cases where the oscillations of the maps become more regular.

Let us now turn to the estimation of the coupling coefficients for an ensemble with symmetric couplings (14), which is significantly more difficult. In addition to the larger number of couplings, the main obstacle is the richness of the system dynamics, consisting in the diversity of oscillatory modes that replace each other when γ changes, multistability, and the existence of dissipative structures [30].

Let us measure $S_{ij}(\gamma)$ with the same $\alpha = 3.95$. Since the system (14) has translational symmetry, all rows of the matrix $\hat{M}$ differ only by a cyclic shift. Therefore, it is sufficient to limit ourselves to measuring the coefficients of only the first row. The graphs $S_{1i}(\gamma)$ $(i = 1, \ldots, 6)$ obtained as a result of the calculations are shown in Fig. 8, *b*. Their appearance indicates a significant heterogeneity of the dependencies, qualitatively different in different ranges of the coupling parameter.

Let us analyze the graphs in Fig. 8, *b*. First of all, we divide the interval into zones with chaotic and regular behavior. For this, we use the Lyapunov characteristic exponents (Fig. 6). The intervals of regular dynamics identified in this way are marked in gray in Fig. 8, *b* (II, IV, VII, and IX). Obviously, it is impossible to measure the directionality in these zones using the method used. However, even in chaotic regions, the qualitative correspondence between the coefficients of the matrices $\hat{S}$ and $\hat{M}$ is not observed everywhere. The smallness of the "zero" coefficients S_{13}, S_{14}, and S_{15} can serve as a criterion here. According to it, good correspondence is observed in zones I and III, where the value of these coefficients does not exceed 1–2 percent, and somewhat worse — in interval V, where these coefficients "grow" up to $\sim$ 5 percent. In the remaining chaotic zones (marked with hatching), there is no correspondence between the influence coefficients and the coupling matrix $\hat{M}$ at all. Obviously, the method does not work in these intervals. The reason for this probably lies in the peculiarity of the system's dynamics,

namely, in the spatial heterogeneity of chaotic oscillations and intermittency observed at large values of symmetric diffusion coupling, which was noted in the work [30]. Verification of this hypothesis requires additional research.

Conclusion

The article considers a method for identifying the structure of connections in a network of chaotic maps using the apparatus of artificial neural networks proposed earlier in the article [26]. It consists of training an ANN to predict the dynamics of an ensemble with simultaneous regularization, during which the neural network adjusts its own structure of synaptic couplings to the structure of couplings of the ensemble. Based on this approach, an algorithm has been developed that allows one to estimate the influence of individual network nodes on its dynamics as a whole, which has been tested on examples of small ensembles of one-dimensional chaotic maps, for which it has demonstrated its effectiveness. In addition to determining the network topology, this approach also allows one to estimate the magnitude of the coupling coefficient.

The conducted studies have shown that the applicability of the method critically depends on the observed oscillatory mode. It works well for the mode of developed spatially homogeneous chaos, is not applicable for regular oscillations and the mode of chaos synchronization, as well as when forming spatial structures in an ensemble.

The effectiveness of the proposed algorithm for analyzing connections between real systems requires additional research. It is determined by such factors as its sensitivity to noise, distortion of the signal shape, the presence of crosstalk, external influences, non-stationarity, etc.

References

1. Cremers J, Hübler A. Construction of differential equations from experimental data. Zeitschrift für Naturforschung A. 1987;42(8):797–802. DOI: 10.1515/zna-1987-0805.
2. Crutchfield JP, McNamara BS. Equations of motion from a data series. Complex Systems. 1987;1(3):417–452.
3. Pavlov AN, Yanson NB. Application of reconstruction method to a cardiogram. Izvestiya VUZ. Applied Nonlinear Dynamics. 1997;5(1):93–108 (in Russian).
4. Anishchenko VS, Pavlov AN. Global reconstruction in application to multichannel communication. Physical Review E. 1998;57(2):2455–2457. DOI: 10.1103/PhysRevE.57.2455.
5. Mukhin DN, Feigin AM, Loskutov EM, Molkov YI. Modified Bayesian approach for the reconstruction of dynamical systems from time series. Physical Review E. 2006;73(3):036211. DOI: 10.1103/PhysRevE.73.036211.
6. Bezruchko BP, Smirnov DA, Zborovsky AV, Sidak EV, Ivanov RN, Bespyatov AB. Reconstruction from time-series and a task of diagnostics. Technologies of living systems. 2007;4(3): 49–56 (in Russian).
7. Takens F. Detecting strange attractors in turbulence. Dynamical Systems and Turbulence. Lect. Notes in Math. 1980;898:366–381. DOI: 10.1007/BFB0091924.
8. Granger CWJ. Investigating causal relations by econometric models and cross-spectral methods. Econometrica. 1969;37(3):424–438. DOI: 10.2307/1912791.
9. Granger CWJ. Testing for causality. A personal viewpoint. Journal of Economic Dynamics and Control. 1980;2:329–352. DOI: 10.1016/0165-1889(80)90069-X.
10. Sysoev IV. Diagnostics of connectivity by chaotic signals of nonlinear systems: solving reverse problems. Saratov: Kubik; 2019. 46 p. (in Russian).
11. Hesse R, Molle E, Arnold M, Schack B. The use of time-variant EEG Granger causality for inspecting directed interdependencies of neural assemblies. Journal of Neuroscience Methods. 2003;124(1):27–44. DOI: 10.1016/S0165-0270(02)00366-7.

12. Bezruchko BP, Ponomarenko VI, Prohorov MD, Smirnov DA, Tass PA. Modeling nonlinear oscillatory systems and diagnostics of coupling between them using chaotic time series analysis: applications in neurophysiology. Physics-Uspekhi. 2008;51:304–310. DOI: 10.1070/PU2008v051n03ABEH006494.
13. Mokhov II, Smirnov DA. Diagnostics of a cause-effect relation between solar activity and the Earth's global surface temperature. Izvestiya, Atmospheric and Oceanic Physics. 2008;44(3):263–272. DOI: 10.1134/S0001433808030018.
14. Mokhov II, Smirnov DA. Empirical estimates of the influence of natural and anthropogenic factors on the global surface temperature. Doklady Earth Sciences. 2009;427(1):798–803. DOI: 10.1134/S1028334X09050201.
15. Sysoev IV, Karavaev AS, Nakonechny PI. Role of model nonlinearity for Granger causality based coupling estimation for pathological tremor. Izvestiya VUZ. Applied Nonlinear Dynamics. 2010;18(4):81–90. DOI: 10.18500/0869-6632-2010-18-4-81-90.
16. Sysoeva MV, Sysoev IV. Mathematical modeling of encephalogram dynamics during epileptic seizure. Technical Physics Letters. 2012;38(2):151–154. DOI: 10.1134/S10637850 12020137.
17. Sysoev IV, Sysoeva MV. Detecting changes in coupling with Granger causality method from time series with fast transient processes. Physica D: Nonlinear Phenomena. 2015;309:9–19. DOI: 10.1016/j.physd.2015.07.005.
18. Chen Y, Rangarajan G, Feng J, Ding M. Analyzing Multiple Nonlinear Time Series with Extended Granger Causality. Physics Letters A. 2004;324(1):26–35. DOI: i10.1016/j.physleta.2004.02.032.
19. Marinazzo D, Pellicoro M, Stramaglia S. Nonlinear parametric model for Granger causality of time series. Physical Review E. 2006;73(6):066216. DOI: 10.1103/PhysRevE.73.066216.
20. Kornilov MV, Sysoev IV. Recovering the Architecture of Links in a Chain of Three Unidirectionally Coupled Systems Using the Granger-Causality Test. Technical Physics Letters. 2018;44(5):445–449. DOI: 10.21883/PJTF.2018.10.46103.17201.
21. Haykin S. Neural Networks. New Jersey: Prentice Hall; 1999. 938 p.
22. Galushkin AI. Neural Networks. The theory basics. Telekom; 2012. 496 p. (in Russian).
23. de Oliveira KA, Vannucci A, Da Silva EC. Using artificial neural networks to forecast chaotic time series. Physica A. 2000;284(1–4):393–404. DOI: 10.1016/S0378-4371(00) 00215-6.
24. Antipov OI, Neganov VA. Neural network prediction and fractal analysis of the chaotic processes in discrete nonlinear systems. Doklady Physics. 2011;56(1):7–9. DOI: 10.1134/S1028335811010034.
25. Shabunin AV. Neural network as a predictor of discrete map dynamics. Izvestiya VUZ. Applied Nonlinear Dynamics. 2014;22(5):58–72. DOI: 10.18500/0869-6632-2014-22-5-58-72.
26. Tank A, Covert I, Foti N, Shojaie A, Fox E. Neural granger causality for nonlinear time Series. arXiv preprint arXiv:1802.05842. 2018.
27. Tihonov AN. On incorrect linear algebra problems and a stable solution method. Reports of the USSR Academy of Sciences. 1965;163(3):591–594.
28. Fujisaka H, Yamada T. Stability theory of synchronized motion in coupled-oscillator systems. Progress of Theoretical Physics. 1983;69(1):32–47. DOI: 10.1143/PTP.69.32.
29. Fujisaka H, Yamada T. Stability theory of synchronized motion in coupled-oscillator systems. The mapping approach. Progress of Theoretical Physics. 1983;70(5):1240–1248. DOI: 10.1143/PTP.70.1240.
30. Shabunin A. Selective properties of diffusive couplings and their influence on spatiotemporal chaos. Chaos. 2021;31(7):073132. DOI: doi.org/10.1063/5.0054510.